Available online at www.sciencedirect.com
SCIENCE DIRECT®
Journal of Sound and Vibration 285 (2005) 669–695
JOURNAL OF SOUND AND VIBRATION
www.elsevier.com/locate/jsvi

Experimental investigation of vibration power flow in thin technical orthotropic plates by the method of vibration intensity

Nirmal Kumar Mandal[a,*], Roslan Abd. Rahman[b], M. Salman Leong[b]

[a]*Centre for Railway Engineering, Central Queensland University, Bruce Highway, Rockhampton, Queensland 4702, Australia*
[b]*Institute of Noise and Vibration, University of Technology Malaysia, Jalan Semarak, 54100 Kuala Lumpur, Malaysia*

Received 8 April 2003; received in revised form 27 January 2004; accepted 26 August 2004
Available online 22 December 2004

Abstract

Vibration intensity technique is used to measure vibration power transmission in thin single layer technical orthotropic plates for flexural waves. Measurement of flexural wave power is carried out in far-field conditions. All measurements are undertaken in the frequency domain using the cross-spectra of acceleration signals, facilitating the use of FFT analyzer. The two-transducer technique applicable to these plates is used for these measurements. Technical orthotropic (rectangular corrugation) plates of steel are used for the measurements. One isotropic plate of steel is also considered for comparison. Method of elastic equivalence technique is used. Both input power and vibration power transmission through the plates are estimated. Far-field power is normalized with the input power for flexural wave. Influence of flexural rigidity on vibration energy transfer is also investigated.

1. Introduction

It is a good practice to control vibration level at the sources. Reduction of input power in structures and its ways to subsequent radiation into the surroundings is of practical interest.

*Corresponding author. Tel.: +617 4930 9287; fax: +617 4930 6984.
E-mail address: n.mandal@cqu.edu.au (N.K. Mandal).

0022-460X/$ - see front matter © 2004 Elsevier Ltd. All rights reserved.
doi:10.1016/j.jsv.2004.08.041

A possible manner may be with the control of transmission of vibration waves along the structures to remote areas. It is thus not only to quantify vibration level but also vibration energy transported along the structures. One method of determining the vibration energy transfer anywhere on the surface of basic structures is to use the vibration power flow concept or vibration intensity.

Structural intensity or vibration intensity technique is a very useful tool for the measurement of vibration power transmission in structures and for controlling of noise and vibration in industries. This method can be successfully used for localization and characterization of sources as well as for identification and ranking of transmission paths of vibration power flow through structures. It is however not possible to get information by experimental modal analysis as it generally deals with the modal parameters such as mode shapes, loss factors, and frequency. Since vibration intensity is a vector, measurement of intensity at a number of points on the structures can be employed to form intensity maps giving pictures of energy flow and locations of vibration source and sink. As a result, this method can practically be used in industries for noise and vibration control introducing proper controlling measures such as isolation of vibration sources and surface damping treatments to the area of most energy transfer in the structures.

Vibration intensity is defined in the solid media, but its measurements can usually be carried out on the surface of the structures. This is because of the fact that in thin structures, the waves propagating through the structures could be reasonably assumed that propagating waves would be parallel to the surface of the structures [1]. Therefore, it is convenient to use the concept of wave-type estimation when addressing the experimental detection of energy flow within the structures. Greater complexity of the mechanical wave field and limited access to the interior of structure bodies, structural vibration implies a higher degree of measurement difficulties as compared to acoustic intensity [2]. This restricts the application of vibration power flow measurements mainly to relatively simple structures such as pipes, beam, and thin plates where propagation of mechanical waves should be considered only parallel to the surface.

Vibration intensity (structural intensity) technique has a unique aspect. It is not dependent on boundary conditions of the structures. This enables to investigate the edge effects of vibration power transmission of pipes, plates and beams. But far-field power flow inherently contains some limitations in selecting measurement points. The measurement points should be away from the boundary and inhomogeneities of the plates. The effects of boundaries and inhomogeneties of the plates are called near-field effects. The near-field effects decay exponentially as function of position and extend to a distance of approximately half the bending wave length from the boundaries and inhomogeneties of the plates [3]. At low frequencies, the disturbing near fields cover a large part of the plate, and valid measurement could be made in the center region only. Far-field concept also enables to use two sensors to determine an intensity vector at a point in the particular direction. The distance between two sensors, called spacing, is selected with regard to bending wave length, such that the ratio of spacing to bending wave length is 0.2 for upper frequency limit and 0.15 for lower frequency limit [4]. The use of this spacing criterion provides an optimal trade off between the reduced finite difference errors afforded by small sensor spacing and reduced sensitivity to standing wave-related errors afforded by larger sensor spacing.

Most of the previous works undertaken on vibration power flow (structural intensity) were related to simple structures, typically beams and plates in flexure using the analysis both in time domain and frequency domain [3,5–9]. Some relevant works in composite materials using this idea

are also available [10–14]. Structural intensity can be computed numerically when predictions of structural behavior in various conditions are needed for complex build-up structures. Vibration intensity, generated by the interaction of dynamic stresses and vibration velocities, for beams and plates can be found by the finite element method [15–17], by statistical energy analysis [18].

Using power flow technique, vibration wave power was also formulated to single-layer naturally orthotropic plates both general and far field condition by flexural wave [19] and by quasi-longitudinal wave [20].

Despite the progress made with respect to both methods and instrumentation, scope exists for further development as work generally had been in the areas of simple beams and thin plates. It is seen from the literature survey that less works have been done on orthotropic materials. Vibration power flow analysis in the area of orthotropic plates (corrugated plates) is very essential for practical reasons. Beam stiffened plates, plate grid structures, corrugated plates are usually used in automotive, ship, aircraft structures. This method gives a clear picture of locations of energy sources and sinks and quantifies energy transmission paths by employing vector maps. Hence it is essential for controlling noise and vibration in industry by incorporating proper damping treatments. Therefore any experimental works on orthotropic plates using structural intensity would give valuable information for noise and vibration control.

2. Basic equations

2.1. Power input to a point

The development of input power and vibration power flow was based on the imaginary part of the cross-spectrum between two signals: between force and acceleration signals at input point for input power and between two acceleration or velocity signals at the measurement locations on the structure for vibration power.

Power input through a point junction either in beams or in plates, for example, could be measured if the force and velocity signals at the point are known. It is conventionally assumed that power injected through a point is only contributed by force. No moment could be transmitted. The following relation of input power could be obtained if the force and motion are in the same direction [7]:

$$P_i(f) = \mathrm{Re}\{G_{vF}(f)\}, \tag{1}$$

where Re is real part and G_{vF} is the cross spectrum of velocity and force signals, and f is the frequency. It is customary to use acceleration signals, a, instead of velocity, v, for practical measurements. By inserting the relationship $v = a/\mathrm{j}\omega$, and using $G_{aF} = G_{Fa}^*$, total active power injected through a point junction by a point force is obtained as [7]

$$P_i = \frac{1}{\omega}\mathrm{Im}\{G_{Fa}\}, \tag{2}$$

where G_{Fa} is the cross-spectrum of force and acceleration signals, Im is the imaginary part, and $\omega(= 2\pi f)$ is the angular frequency. If a force is applied to a point on the plate in the direction perpendicular to the plane of plate, Eq. (2) could be valid for flexural waves. On the other hand, if

it is applied to a point along the pane of the plate, the same Eq. (2) could also be valid for longitudinal waves. By putting the value of ω in Eq. (2), it is possible to get input power equation in terms of frequency, f.

$$P_i = \frac{0.159}{f}\mathrm{Im}\{G_{Fa}\}. \tag{3}$$

The imaginary part of the cross-spectrum of Eq. (3) could be achieved from the FFT analyzer and after post-processing using Matlab or MS Excel, the input power P_i (W/Hz) could be computed. Eqs. (2) or (3) is valid for both isotropic and orthotropic plates.

2.2. Far-field power

The idea of far-field power was first defined by Noiseux [3]. Approximately one-half of a flexural wave length far from the edges and discontinuities of structures, the exponentially decaying near-field components are negligible and flexural wave field consists of free propagating waves. This idea is called far-field conditions. The far-field condition simplifies structural intensity estimation. In isotropic plates, two components of active power from shear force (P_s) and moment (P_M) are equal [3]. The total active power (P_T) could thus be obtained by estimating only one component such as

$$P_T(f) = 2\mathrm{Re}\{G_{VQ}\}, \tag{4}$$

where G_{VQ} is the cross-spectrum of velocity and shear force signals. The far-field power in simple beams and isotropic plates had been established and only one cross-spectrum is sufficient to obtain this power. This is in fact the 'two-transducer' method [3,5,7]. For isotropic plates, the far-field power, also called time-averaged power or active power, could be obtained as [7]

$$I = \frac{2\sqrt{Dm''}}{d\omega^2}\mathrm{Im}\{G_{12}\}, \tag{5}$$

where I is the intensity (far-field power, P_T) in the direction of the transducer pair from 2 to 1 as in Fig. 1, d is spacing of the accelerometers, D is flexural rigidity of the plate, m'' is the mass per unit

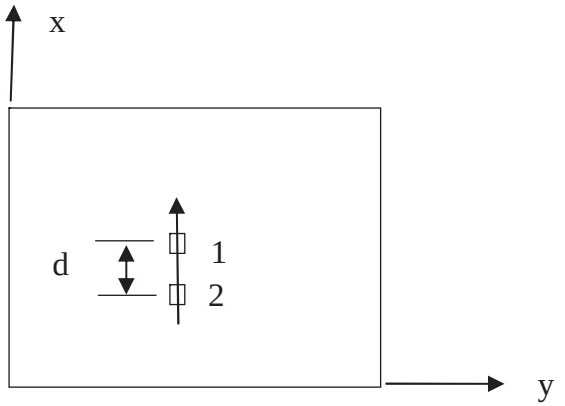

Fig. 1. Coordinate system of plate along with two-point transducer array.

area of the plate, G_{12} is the cross-spectrum of acceleration signals, and Im{ } is imaginary part. Eq. (5) is applicable both in x- and y-directions of the plate (Fig. 1).

The imaginary part of the complex power, called reactive power, is defined as the standing wave power per unit width or it can be described alternately as that portion of the energy which resides in the stationary waves and is, essentially, stored within the medium [21].

By normalizing the power flow at the far-field conditions with respect to input power at a point source, power ratio, R, for two transducer method could be found by taking the ratio of Eqs. (2)–(5)

$$R = \frac{2\sqrt{Dm''}}{d\omega} \frac{\mathrm{Im}\{G_{12}\}}{\mathrm{Im}\{G_{Fa}\}}. \tag{6}$$

In a logarithmic format (in decibels), the power ratio could be shown by making the difference between the far-field power and input power [22]

$$R(dB) = 20\log_{10}(|R|) = 20(\log_{10}|I| - \log_{10}(|P_i|). \tag{7}$$

The flexural wave power, in naturally orthotropic plates, can be obtained using finite difference approximation. Recently, a measurement method for quantify power flow in naturally orthotropic plates has been developed [19] and is presented below as

$$I_x(f) = \frac{2\sqrt{D_x m''}}{d\omega^2} \mathrm{Im}\{G_{12}\}, \tag{8}$$

where G_{12} is the cross-spectrum of the acceleration signals at points 1 and 2, and D_x is the flexural rigidity of the plate in x-direction. This relation presents the flow of vibration power in orthotropic plates in the x-direction from point 2 to 1 (Fig. 1). The y-component of this power could be obtained by interchanging the x- and y-axis in Eq. (8).

The cross-spectrum of two acceleration signals could be measured directly by multi-channel FFT analyzer using two accelerometers. An estimate of it can however be found using frequency response method with one transducer technique [7], as a result phase errors are reduced. Only one cross-spectrum of acceleration signal is required to obtain the total power. This is a new definition of structural intensity that also illustrates the power flowing per unit width of the plate (W/m). Normalizing power flow, R, of this plate for far-field conditions could be found similarly by taking the ratio of Eqs. (2)–(8). The imaginary part or reactive part of complex power in flexural wave may be obtained using auto-spectra of field signals of velocity or acceleration [19].

3. Experimental studies of flexural wave power

Estimation of time average vibration power input and far-field power in isotropic plate and orthotropic plates has been carried out. The work as carried out in this study focuses on the flow of energy due to flexural waves since this mode contains most of the structure-borne sound. In solid materials, the mechanical vibration propagates by three characteristics modes or wave types—flexural, longitudinal (compression) and shear waves [23]. Some wave types, such as flexural exhibits dispersion where the propagation speed is not constant but varies as a function of

frequency. Dispersion implies that the speed of the wave propagation (phase velocity) differs from the propagation speed of energy transmitted by the wave (group velocity) [2].

In this paper, established two-transducer method (Eq. (6)) and input power (Eq. (2)) are used first in isotropic plate for verifying test rig and method applied by comparing the results with those established earlier by different authors. Then measurement method applicable for naturally orthotropic plate [19] is used to quantify flexural wave energy transfer in technically orthotropic plates using the method of elastic equivalence [24].

In the following section, estimation of far-field power and determination of other related data in the frequency domain for isotropic plate are presented.

3.1. Methodology and verification of results in isotropic plate

Laboratory experiments are undertaken with the objectives of measuring and comparing the flexural wave power in far-field conditions of different plates with different rigidity. Direct power input to a point of the plates is measured with a force transducer and an accelerometer placed in a same point opposite to the force transducer. A constant force signal was applied through out the experiments for all plates and which was monitored constantly.

The schematic diagram and its instrumentation of the laboratory test rig for the measurement of flexural wave power on steel isotropic plate were fabricated as in Fig. 2. At the upper end of the plate, a mini-shaker (B&K type 4810) was used to provide random white noise excitation to the

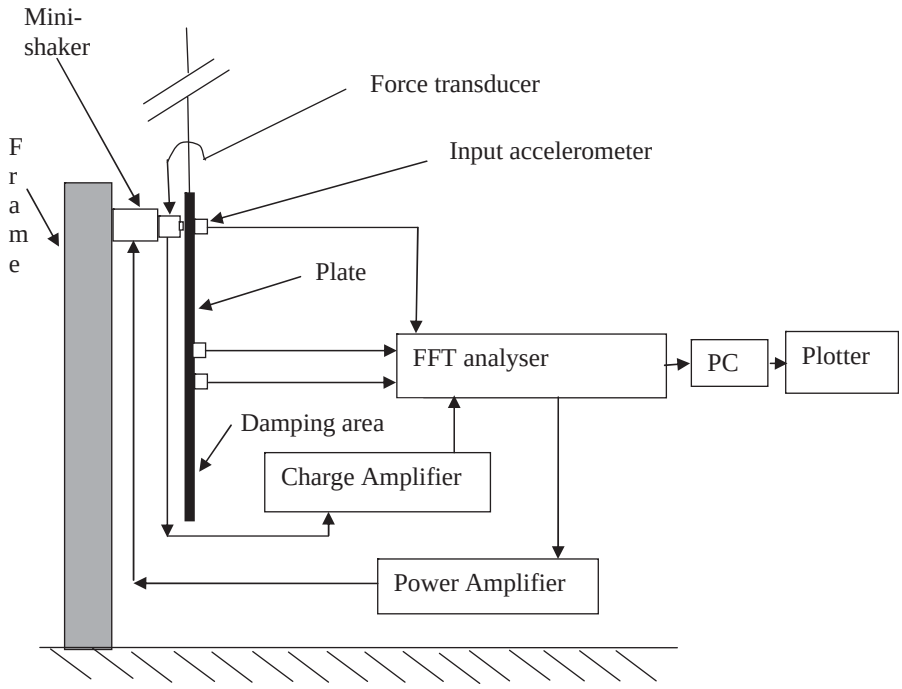

Fig. 2. Test rig and instrumentation of a freely suspended plate excited by a mini-shaker at one end and heavily damped at the other end, with indicating the locations of force transducer and different accelerometers (input and far field).

plate through force transducer (B&K type 8200). Two accelerometers mounted away from the source and boundaries were used to measure far-field power. The major components of instrumentation were the miniature accelerometers (piezoelectric, ICP, with an effective mass of 1.7 gm) and multi-channel FFT analyzer (HP 35670A). The accelerometers were mounted on the plate with bee wax. The mini-shaker was driven by internal noise source of the FFT analyzer. The standard data files (SDF) of the measurement were transferred from analyzer to a PC for post processing, and the results were plotted by a plotter.

The sides of the square isotropic plate (Fig. 3) are 0.90 m and its thickness is 0.8 mm. The material properties such as Young's modulus and Poisson's ratio are 162.8 GPa and 0.31, respectively. With these plate dimensions and material properties, it can be expected the far-field condition (at least half a wave length from the boundaries and source) at the center of the plate at frequency from about 9.12 Hz upwards. Upper frequency limit for flexural wave to be valid (wave length equal to six times the thickness of the plate [23]) was 320.7 kHz. The spacing of the accelerometer positions should be as short as possible so as to minimize finite difference error, but too short distance causes random error. The spacing, d, was chosen rather arbitrarily to be 20 mm. The spectral bandwidth was set at 800 Hz. At the upper frequency limit of 800 Hz, the wavelength was calculated to be 96.10 mm (calculations of wavelength are presented in Appendix A). Thus the accelerometer spacing is approximately 1/4.8 of the wavelength.

The plate was freely suspended vertically using steel strings at two points and the lower part was damped heavily by the spongy-foam and sand (Fig. 3). This type of damping is usually provided at the end of the test object to suppress the reflections. Other substances used for this purpose are plastics, adhesive tape sheet and many similar other things. The effectiveness of damping

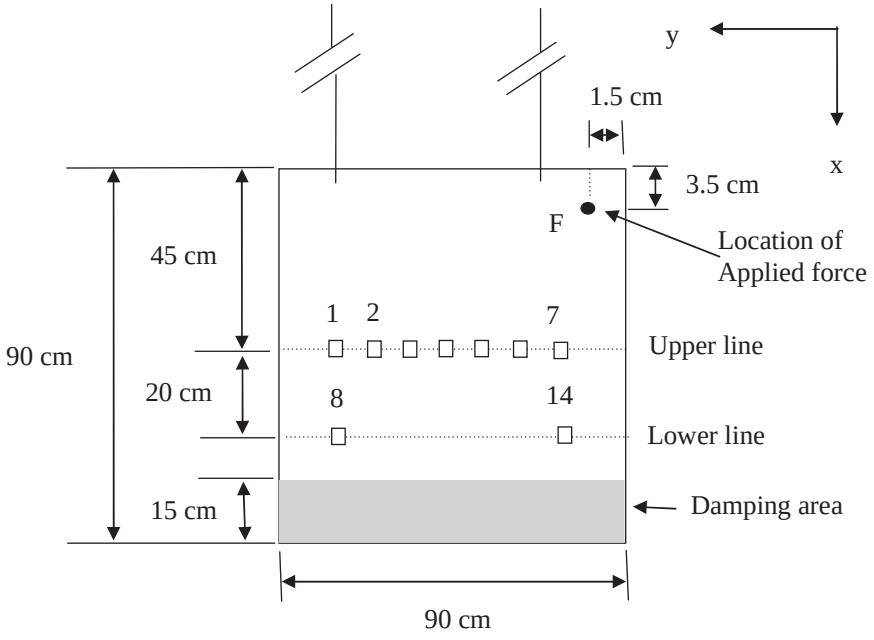

Fig. 3. Different measurement points on two measuring lines (seven on each line), indicating locations of applied force and damping on plate.

materials was tested by measuring the response of the plate with or without the use of damping materials. Vibration fields without damping materials would result in a reverberant plate as vibration energy reflects back and forth in the plates. Initially less damping area was considered and gradually it was increased until a stable vibration field was achieved [25]. This ensures that a reverberation condition was less obvious. If it is not so, phase mismatch would give some random error as a result of which coherence values would be away from unity [2,7]. The coherence graphs (Figs. 4, 13 and 14) illustrate that random error is not a problem. Such type of measurement to ensure effectiveness of damping material could be found in the literature [25].

The suspension and force injection were carefully tested in order to minimize the generation of vertical and torsional motion of the plates, which could disturb the true detection of lateral horizontal motions. A calibration test of the entire measurement chain was undertaken before the actual measurements. The key components of these measurements, such as force transducer, accelerometer and others, were tested and calibrated separately. Repeatability was checked and errors were less than 2% in the frequency range of interest.

In the measurements, mainly the imaginary part of cross-spectrum between two accelerometer's signals at the far field (as required by Eqs. (5) and (8)) and the same between force and acceleration at the excitation point (as required by Eq. (2)) was measured. The mini-shaker, providing random white noise, was connected to internal noise source of the FFT analyzer. White noise commonly known as random excitation is constant in magnitude over frequency range. For the measurements of cross-spectrum between two acceleration signals for all fourteen points in the far fields (Fig. 3), a fixed array of transducers was used for all points rather than moving a transducer sequentially between the array locations. Under such an arrangement, a stationary field was made during data acquisition of cross-spectral. The FFT analyzer was used to collect typically 200 ensemble averages of the cross-spectra, auto-spectra and coherence functions needed in the subsequent processing.

Example of coherence functions observed during data acquisitions in steel isotropic plate is shown in Fig. 4 with the frequency resolution of 1 Hz approximately. Some lack of coherence

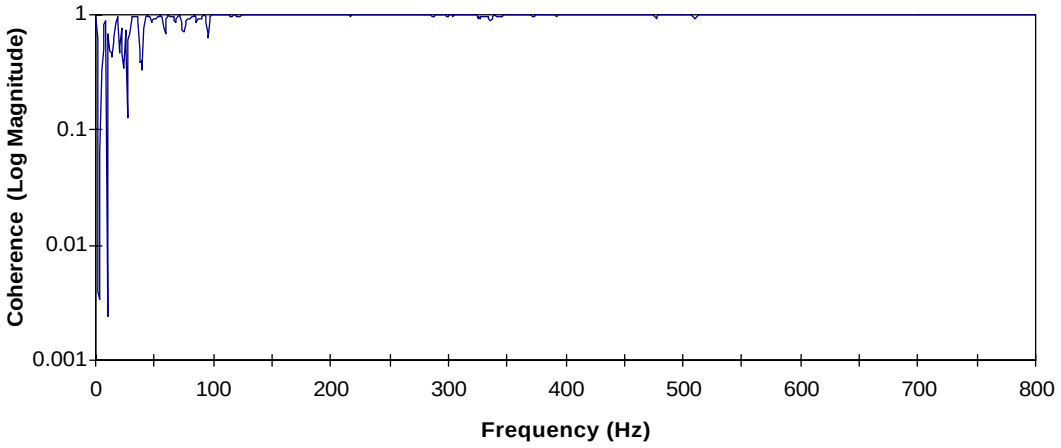

Fig. 4. Coherence function between force and acceleration at the input point.

occurred at the low frequencies, it was deemed to be acceptable on over all basis [7,22]. A more sufficient spectral resolution may improve coherence values at those frequencies.

Fig. 5 shows the power spectrum of input force. It is observed that there is a peak approximately at 800 Hz. This peak may be due to nonlinearity and/or other extraneous noise effective at this frequency. The linear magnitude of force signal was also measured in a lower frequency, Fig. 6. This figure shows a stable magnitude all over the frequency range. In Fig. 7, driving point acceleration is presented and it is observed that the lowest part of frequency is more damped. The imaginary part of cross-spectrum of force and acceleration at input and the imaginary parts of cross-spectrum between two acceleration signals at various measurement locations (Fig. 3) were used to compute input power and far-field power using Excel program. Real part of cross-spectrum between force and acceleration at input and between the acceleration signals at far field may give useful information regarding standing energy stored in the structures.

Measurement of vibration intensity on beams can usually be performed by inserting transducers in a four-point or two-point array in one location. But one location measurement results very raw information of energy transmission in case of plates. It is generally considered to be point grid random in nature or along different lines (Fig. 3) on the plates [2]. Estimates for net power through the measurement line grid were constructed as a line integral (by calculating the average) of the normal components of the properly scaled intensity vectors. Total power transferring through a line grid could be obtained as

$$I_{\text{total}} = \int_L \vec{I} \cdot \vec{n}\, \mathrm{d}L, \tag{9}$$

where $\vec{I}$ is the intensity vector and $\vec{n}$ is the unit normal vector perpendicular to the line. Average power could be computed from total power taking into account the number of measurement points on each line (Fig. 3). Proper scaling of intensity vector is necessary due to the fact that the

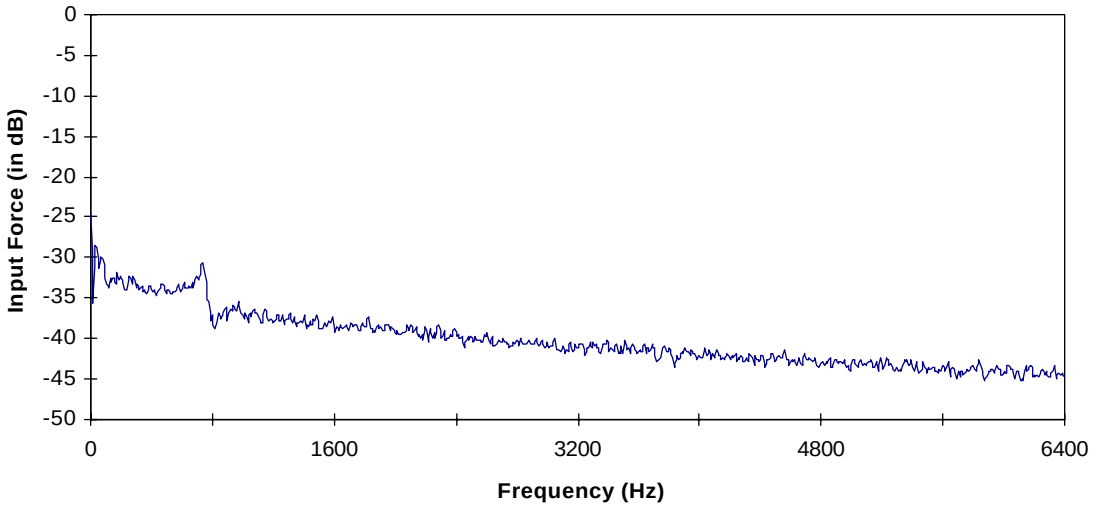

Fig. 5. Power spectrum of random force signal measured by force transducer in dB.

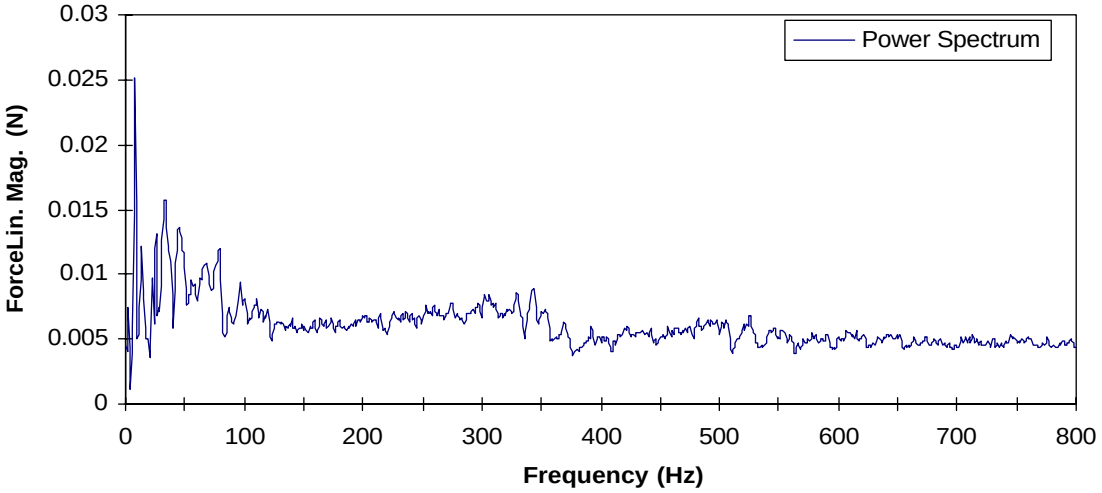

Fig. 6. Random force signal for low frequency range measured by force transducer.

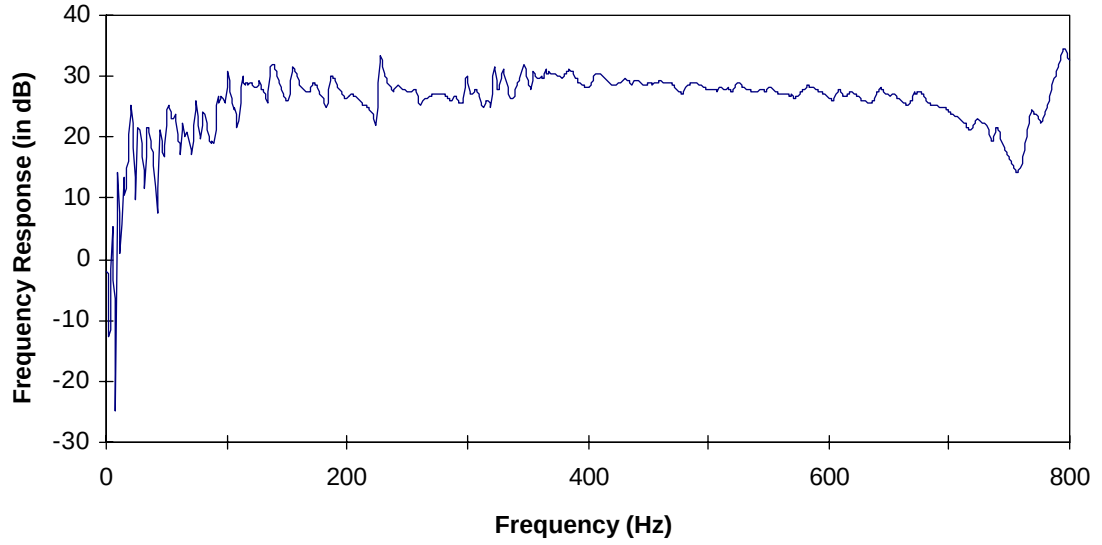

Fig. 7. Driving point acceleration (acceleration/force at input) in dB, frequency resolution of 1 Hz.

units of input power and intensity are W and W/m, respectively [7]. When intensity is to compare with input power, it is necessary to make same unit of both quantities. Here the unit W was considered for both quantities and it was managed using Excel program. There are three ways of comparing normalized power: ratio form (Eq. (6) and Fig. 20 for example), superposition (Fig. 17 for example), and subtraction (not considered).

Normalized power of input power and far-field power for the isotropic plate is shown in Figs. 8–10. Measurement locations were chosen such that all points in two lines (Fig. 3) were in the far-field except at the injection point. It should be reasonably sound to expect that the far-field

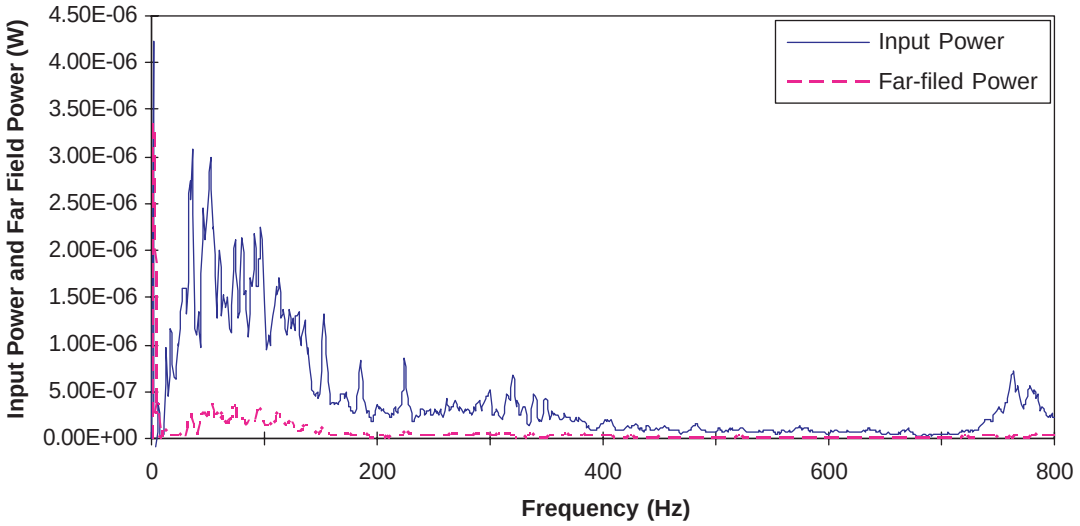

Fig. 8. Normalized input and far-field power from upper measurement line for isotropic plate, frequency resolution of 1 Hz.

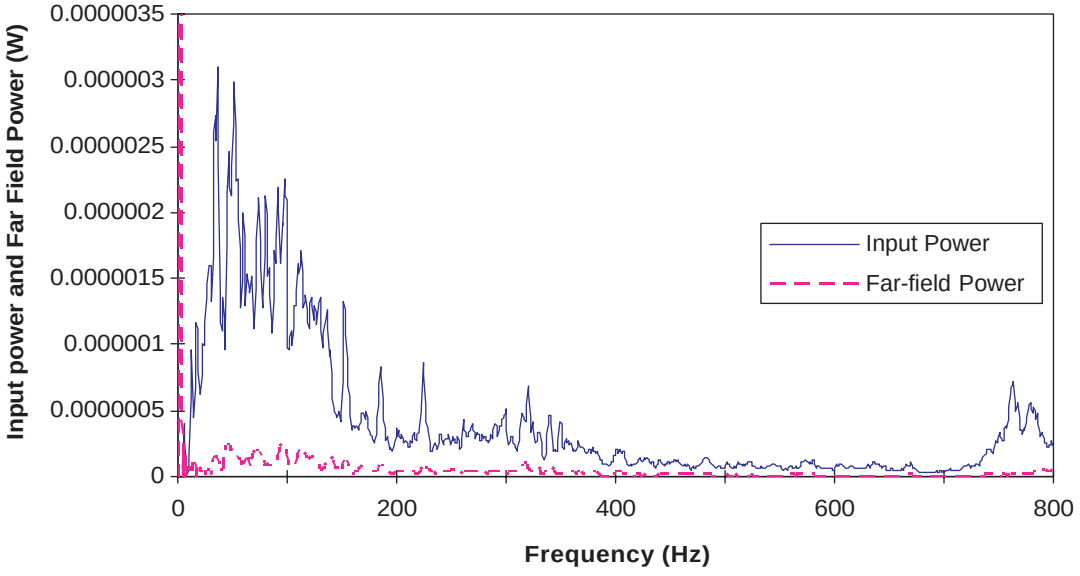

Fig. 9. Normalized input and far-field power from lower measurement line for isotropic plate, frequency resolution of 1 Hz.

power must be less than the input power [22]. This is supported by the observations in Fig. 8–10. Far-field power was also compared considering the energy transfer from two measurement lines and it is shown in Fig. 11. The graphs in Figs. 8–11 show similar pattern to the results available in the literature [2,7,8,22] and hence it can accepted and verified the measurement methodology, test

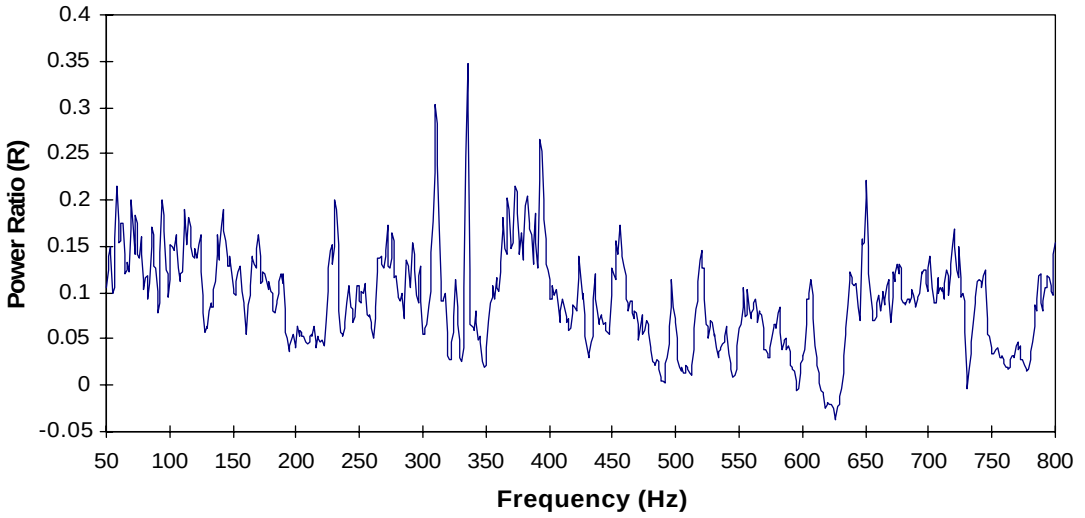

Fig. 10. Power ratio of far-field power from upper measurement line and input power for isotropic plate.

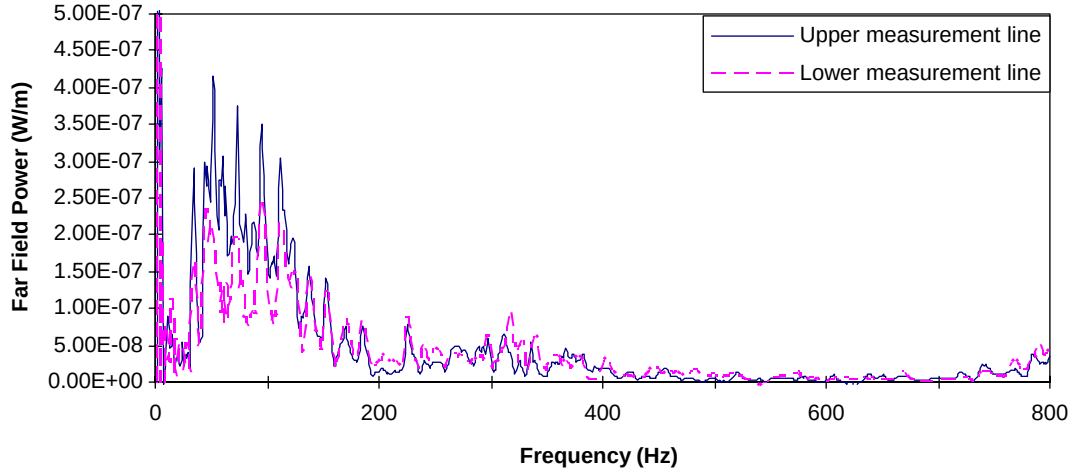

Fig. 11. Far-field power measured from isotropic plate for upper and lower measurement line, frequency resolution of 1 Hz.

rig, and instrumentation. Thus it can be suitable for measurement of far-field energy transfer in orthotropic plates.

3.2. *Far-field power flow through technically orthotropic plates*

In this study, two rectangular corrugated plates, one small and the other big, were considered. These plates were fabricated from isotropic steel plate. Due to the geometrical modifications, these plates are no longer isotropic in nature, and are therefore technical orthotropic plates. If the material properties of a plate are different in orthogonal directions, the plate is called natural

orthotropic and its thickness is uniform. One repeating section of both corrugated plates is shown in Fig. 12 and its characteristic dimensions are shown in Table 1. The sizes of small and big rectangular corrugated plates were same like isotropic plate such that all sides were 0.9 m and thickness of the equivalent plate was 0.8 mm.

In isotropic plates, far-field power could be estimated by two-point transducer method and general field power by a transducer array of eight points [3,5]. In the case of orthotropic plates, a new model is necessary. Recently, a structural intensity method for naturally orthotropic plates has been developed [19]. This method (Eq. (8)) is used in the present study of corrugated plates

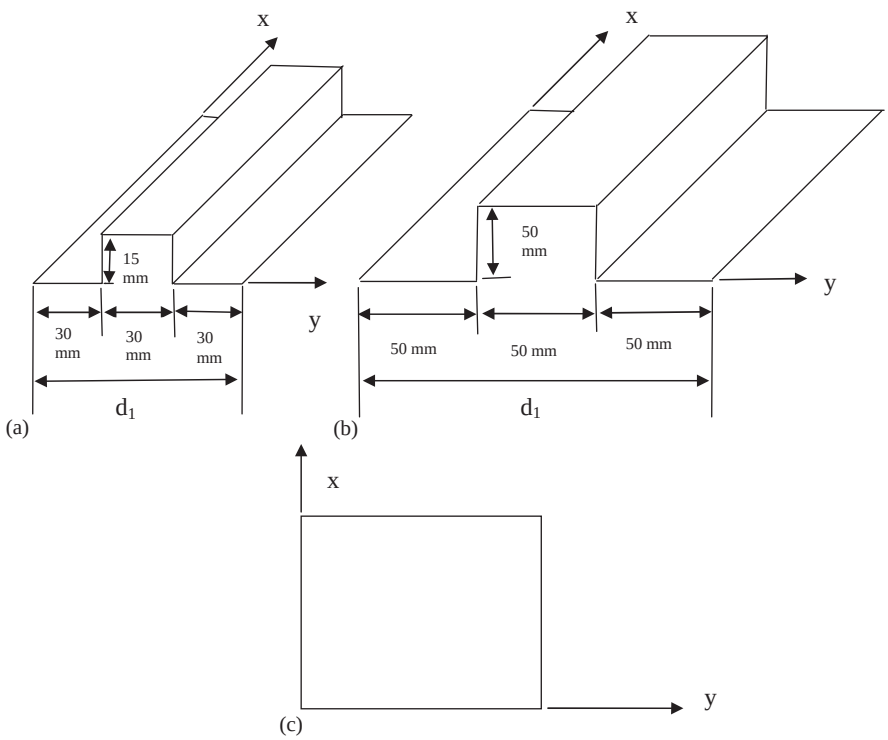

Fig. 12. Physical dimensions of one repeating section of rectangular corrugated plates (a) for small, (b) for big, and (c) for equivalent plate (all plates 0.9 m × 0.90 m square).

Table 1
Physical dimensions of one repeating section of small and big rectangular corrugated plate

Physical quantities/types of plates	Rectangular corrugated plate	
	Small	Big
Length of one repeating section, d_1 (in mm)	90	150
Actual flat length of one repeating section, s (in mm)	120	250
Number of repeating sections	10	6

using the method of elastic equivalence [24]. The elastic equivalence technique models corrugated plates to a plate of uniform thickness (Fig. 12c) by defining different rigidities. Now this equivalent uniform thickness plate is considered to be a naturally orthotropic plate and Eq. (8) can be used.

If the spectral frequency is set at 800 Hz and with the geometric dimensions and material properties of the plates, it could be computed that the flexural wavelengths are to be 507.04 mm for small rectangular corrugated plate and 902.34 mm for big rectangular corrugated plate. Both flexural wavelengths are significantly greater than the characteristic dimension d_1 of the repeating section of the corrugated plates. This condition ensures the flexural wave transmission in corrugated plates [23] (calculation of wavelength for all plate is given in Appendix A).

Both rectangular corrugated plates were suspended freely as in Fig. 3 such that the x-axis is parallel to the direction of corrugation (Fig. 12). As a result the flexural rigidity in x-direction of the plates, D_x, is greater than that of D_y. Spongy-foam and sand was provided at the lower part of the plates, as in the case of isotropic plate, as a damping material so as to suppress the reflections of wave and making strong energy transfer in positive x-direction or in the direction towards damping material. In every plates, like isotropic, two measurement lines were considered where different points were located as in Fig. 3. Only a small change was made for the measurement of energy transfer in big rectangular corrugated plate. It is due to different characteristic dimension d_1 of it. The distance between the measurement point and the distance of extreme points to the nearest edges of the plates are given in Table 2.

Flexural wavelengths for both small and big corrugated plates have increased significantly compared to that of isotropic plate. It was due to increase of rigidity in one direction as a result of corrugation. The order of increase in rigidity in these plates was expected to be approximately 10^3 or even more [26]. The far field, the half of the flexural wavelength away form the boundary [3], requires larger area of the plates, resulting in a less area for measurements. For practical structural intensity measurements, it could be possible to measure in an area as close as one-tenth of the wavelength from the boundaries with good results [27]. Now, enough area was therefore available for measurements. The distance between the measurement points, the spacing d, was chosen again to be 20 mm. The accelerometer spacing was thus approximately $\frac{1}{25}$ of the flexural wavelength for small rectangular corrugated plate and $\frac{1}{45}$ for big rectangular corrugated plate. Due to this short transducer spacing compared to wavelength, the possibility of finite difference errors occurring was very small [7]. This ratio of spacing to wavelength may cause standing wave-related error to

Table 2
Different significant dimensions relating to measurement of all plates

Plates/parameters	Isotropic plate	Small rectangular corrugated plate	Big rectangular corrugated plate
Distance between measurement points, mm	90	90	75
Distance of extreme points to the edge, mm	180	180	225
Measurement lines	2	2	2
Number of points	14	14	14

occur [4]. As strong damping was provided to the plates and it was found that a stable condition occurred in vibration fields. It may be argued that as reflections and scatterings are less, there is less chance of resulting error being sensitive to standing waves (more on 'discussion' section).

The measurement chain was mainly the same as it was in the case of isotropic plate illustrated in the Section 3.1. The imaginary part of the cross-spectra between two acceleration signals in the far field and between force and acceleration signals at injection point was measured by FFT analyzer for subsequent calculation of far-field power and input power for rectangular corrugated plates as required by the Eqs. (2) and (8) respectively. The mini-shaker provided same random white noise from the internal noise source of the analyzer. A fixed array of transducer was used and the FFT analyzer was used to collect typically 200 ensemble averages of the cross-spectra, coherence and frequency response functions.

Typical examples of result of energy transfer and related data for small and big rectangular corrugated plates are hereafter given. Examples of coherence functions for these plates are shown in Figs. 13 and 14, and corresponding driving point accelerations in Figs. 15 and 16.

Input power and far-field power for both small and big corrugated plates were estimated. The far-field power was normalized to input power to facilitate comparison of the results and the method. This is possible because the same measurement state was used in all plate models for input force to ensure a constant and repeatable condition. For small rectangular plate, Figs. 17 and 18 show normalized far-field power to input power, Fig. 19 for far-field power from two measurement lines and Figs. 20 and 21 for power ratio, R.

For a big rectangular corrugated plate, on the other hand, the same method was used for data acquisition and analysis. Spectral resolution was increased to 4 Hz for calculation of energy transfer. Figs. 22 and 23 show normalized far-field power to input power and Fig. 24 shows up the relative energy transfer considering two measurement lines.

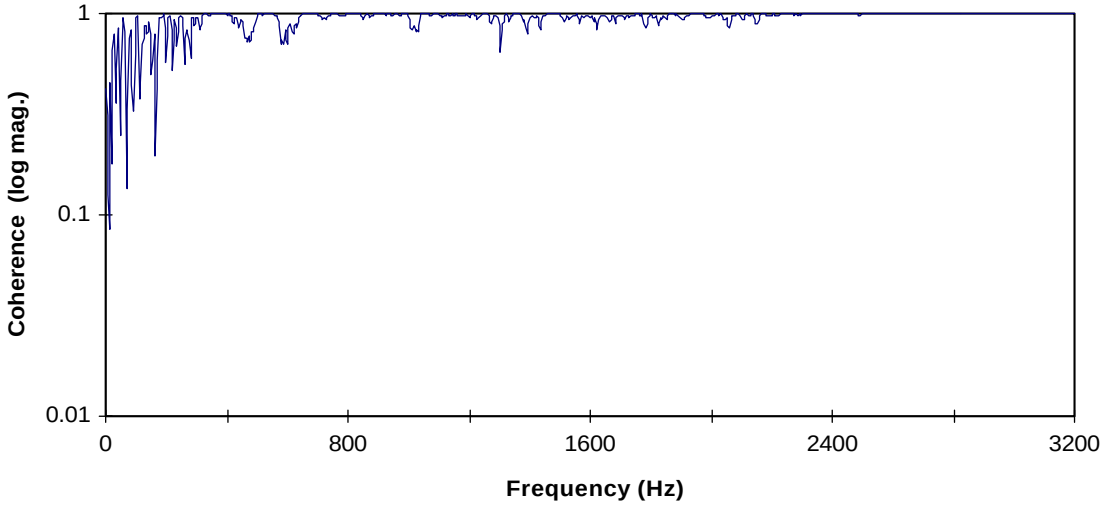

Fig. 13. Coherence function between force and acceleration at input point for small rectangular corrugated plate (SRCP), resolution of 4 Hz.

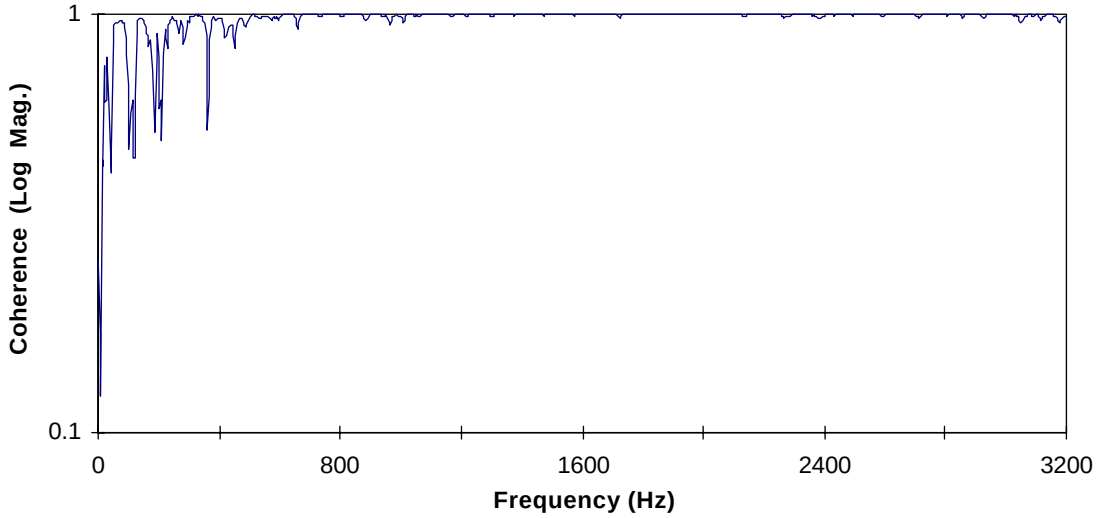

Fig. 14. Coherence function between force and acceleration at input point for Big rectangular corrugated plate (BRCP), resolution of 4 Hz.

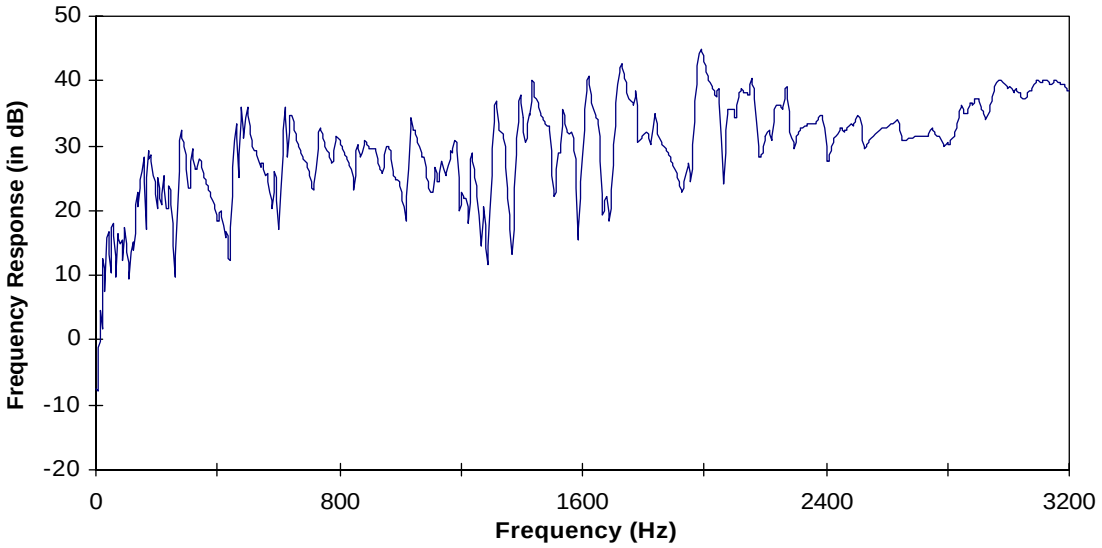

Fig. 15. Driving point acceleration for SRCP at input, resolution of 4 Hz.

4. Discussions

An experimental study was undertaken to verify and prove the soundness of the method developed for measuring vibration power flow in orthotropic plates for flexural waves. Corrugated plates were considered for this purpose. Three plate models are considered. Of them, one is an isotropic plate and the other two are rectangular corrugated plates, one small and

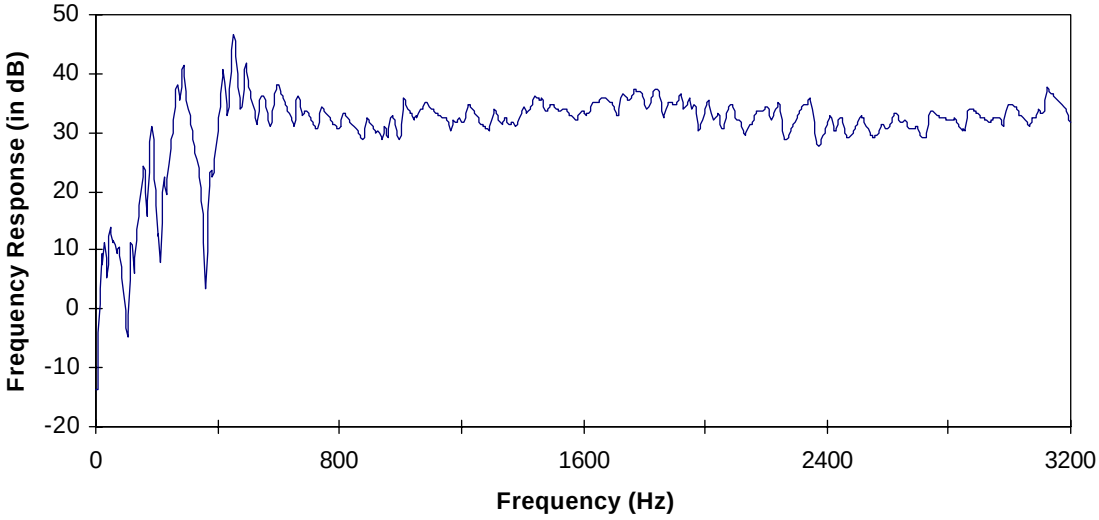

Fig. 16. Driving point acceleration for BRCP at input, resolution of 4 Hz.

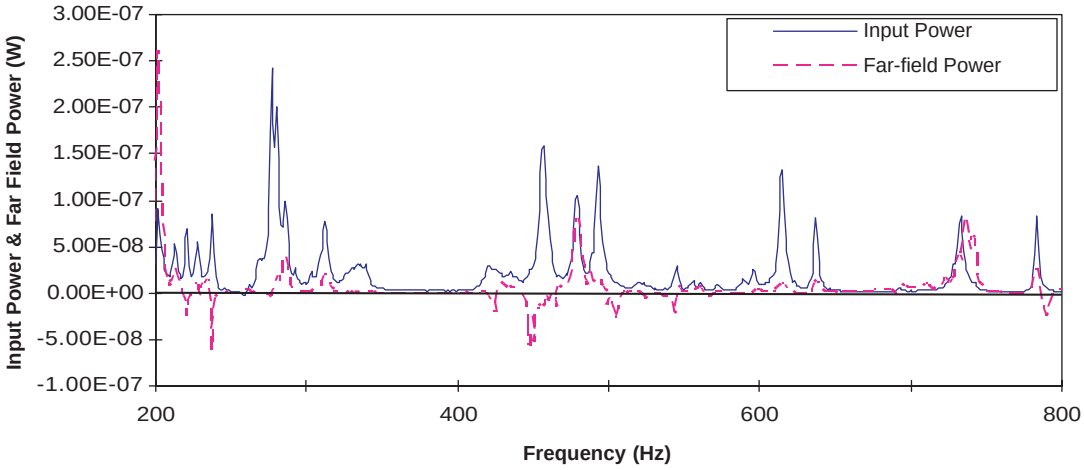

Fig. 17. Normalized far-field power and input power form SRCP from upper measurement line, frequency resolution of 1 Hz.

the other big. Shape and size of the plates are described in the last section. The isotropic plate was used to verify the measurement methodology and test rig used for subsequent measurement on orthotropic plates. In this study, input power and far-field power are measured along with other frequency response functions such as power spectrum, coherence function and driving point acceleration. The corrugated plates are considered in this study because these types of plate are widely used in industries. They are in the category of technically orthotropic plate [24]. The measurement model [19] considered here was applicable to naturally orthotropic plates of uniform

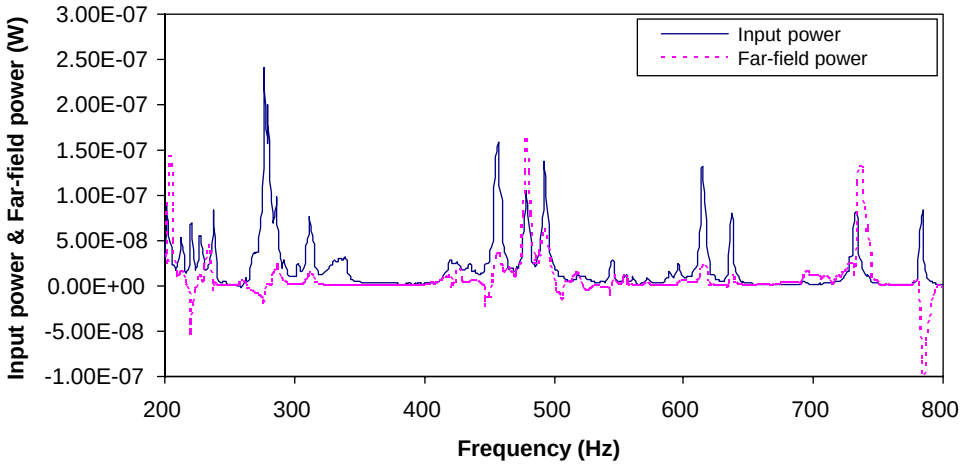

Fig. 18. Normalized far-field power and input power form SRCP from lower measurement line, frequency resolution of 1 Hz.

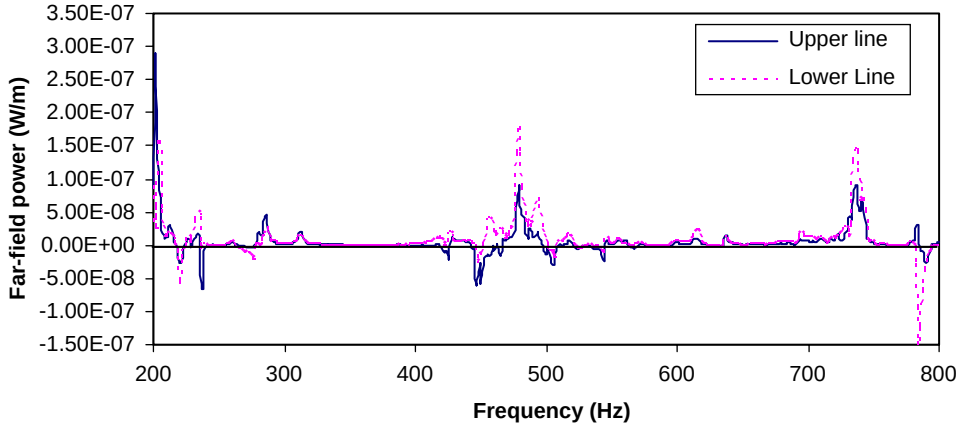

Fig. 19. Far-field power for SRCP from both upper and lower measurement lines, frequency resolution of 1 Hz.

thickness. Method of elastic equivalence [24,28–31] was applied to corrugated plates to get an equivalent plate of uniform thickness by defining proper rigidity constants. Power flow model as applicable for naturally orthotropic plates could be used on technically orthotropic plates with reasonable accuracy [31].

Coupling of different waves are a major problem especially in complex structures. Structural intensity can be computed numerically when predictions of structural behavior in various conditions are needed for complex build-up structures. But in this paper, an alternate way was considered. Using the method of elastic equivalence, the corrugated plate was transferred to a plate of uniform thickness that behaves like a simple structure. As a result, coupling does not create a problem.

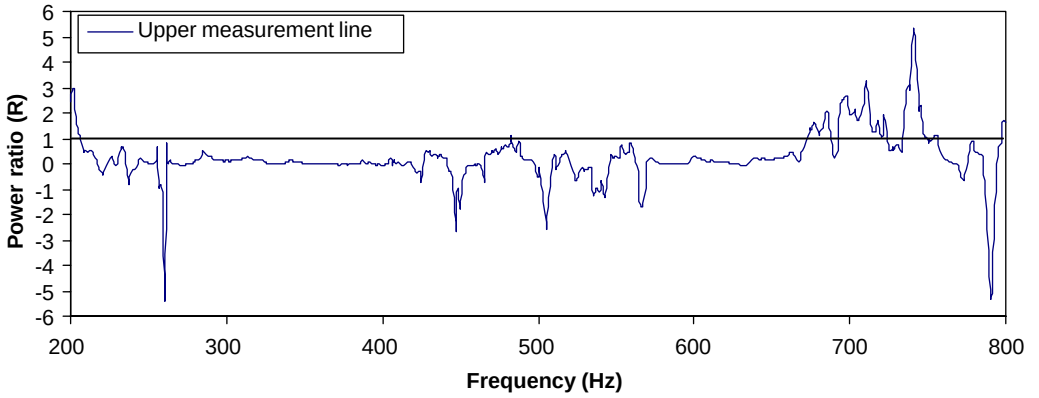

Fig. 20. Power ratio of far-field power to input power for SRCP, frequency resolution of 1 Hz.

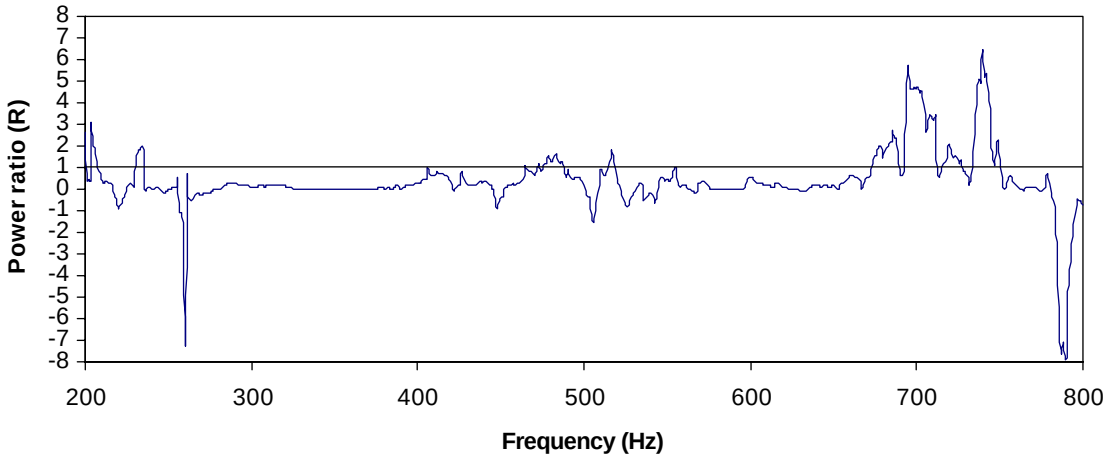

Fig. 21. Power ratio of far-field power to input power for SRCP, (lower measurement line) frequency resolution of 1 Hz.

The standard way of providing the soundness of any method and technique in structural intensity is to normalize vibration power transmission in structures to input power injected in it [7,8]. Under all conditions, it is expected that input power must be greater than the vibration power flowing [22] for identical conditions on same structure. In some cases, vibration power may however exceed the input power and power ratio between far-field power and input power on the same plate is greater than unity [7,8,22]. In Figs. 8 and 9, the normalized far-field power (W) to input power in isotropic plate is plotted. In all respects, it is observed that the input power to the plate has a higher value than that of the far-field power. This is confirmed from Fig. 10 for example. Power ratio in this figure shows that it does not exceed the value of unity, but have some negative values in some frequencies. The far-field power in these frequencies has negative amplitudes and thereby yields negative power ratio.

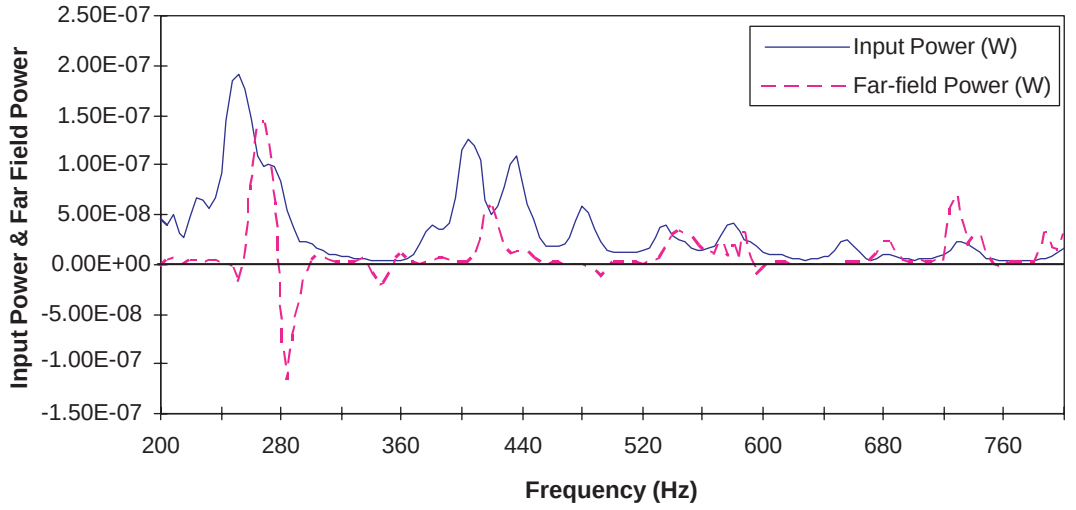

Fig. 22. Normalized far-field power to input power for BRCP from upper measurement line, frequency resolution of 4 Hz.

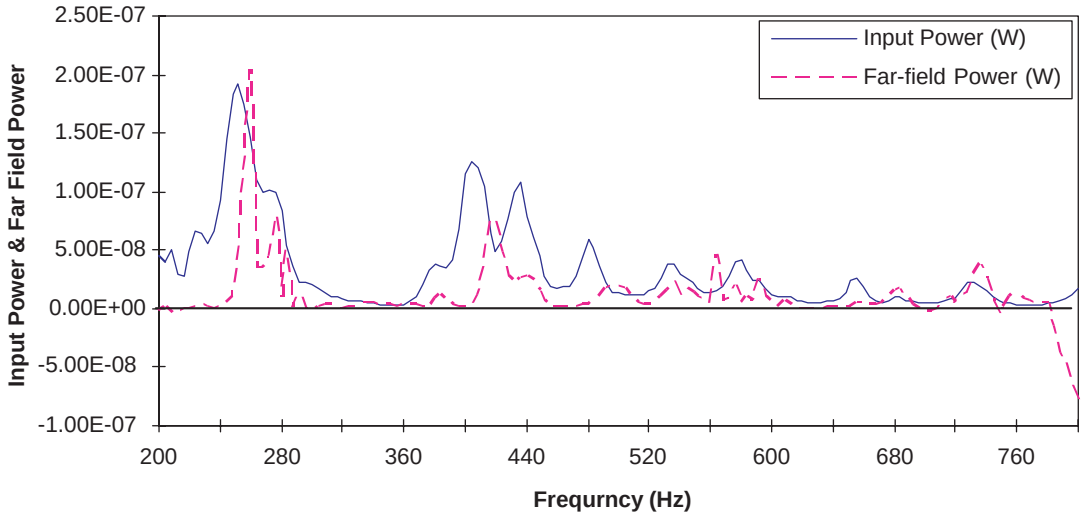

Fig. 23. Normalized far-field power to input power for BRCP from lower measurement line, frequency resolution of 4 Hz.

Three types of power flow pattern [32] are observed: straight type, S-shaped type and vortex type. Among them, S-shaped type and vortex type flow pattern may play important roles for energy transfer especially in making negatives loops. These patterns are also applicable to in-plane waves. Even it is true for acoustic intensity [32]. Due to this effect and reflections from edges, negative structural intensity values do occur especially in two-dimensional structures. The

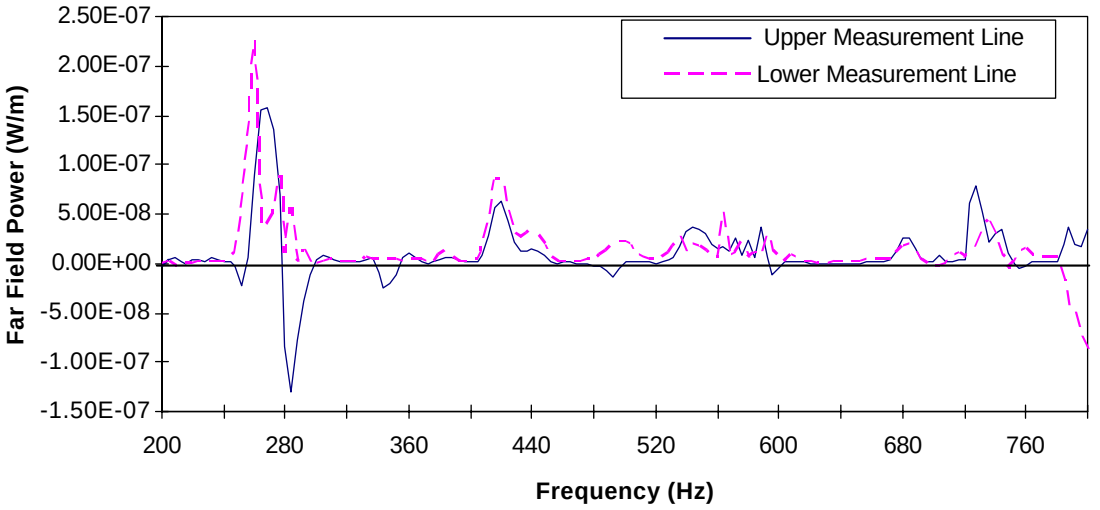

Fig. 24. Far-field power for BRCP from two measurement lines, frequency resolution of 4 Hz.

magnitude of the negative peaks could be reduced by introducing more damping area not only in lower side but also to the other vertical sides (Fig. 3).

In the case of orthotropic plates, far-field power was normalized to the input power injected to these plates for facilitating comparison of the results. Figs. 17, 18, 20 and 21 show this comparison for small rectangular corrugated plate and Figs. 22 and 23 for big rectangular corrugated plate. The graphs of all figures confirm that the input power always exceeds the far-field power, with some exceptions. In some frequency range, typically at higher range, far-field power has a higher value than input power. The use of more measurement points on a measurement line may resolve this anomaly. Reflections and scatterings of waves from edges of the plates (only lower side of the plates is damped) and rotational (vortex) characteristics of power flow field create additional influence on far-field power to be greater than input power and yielding negative values. However, the characteristics of the results are consistent with the result reported in the literature [7,8,22]. The plots of power ratio of these plates (Figs. 20 and 21) ensure this nature in a more convenient way. In the region closer to damping area, reflections of wave are less, with strong power flow as expected occurring in the direction towards damping area (Figs. 11,19 and 24).

The errors in measurements are quite inherent. Good measurement method and instrumentation give results of higher accuracy. The spacing between the sensors was chosen rather arbitrary. A spacing of 20 mm was used, representing approximately $\frac{1}{45}$ wavelength for one plate, stated before. The smaller is the spacing of the sensors, the lower will be the finite difference error of the measurements [4]. The finite difference errors start to appear if the spacing is greater than $\frac{1}{5}$ of wavelength [7]. The ratio of spacing and wavelength of this study ensures a good accuracy in terms of finite difference errors. On the other hand, this ratio between the spacing and the wavelength may give some phase mismatch of the sensors which provides some random errors. Random errors may further occur due to amplitude and imperfect positioning of sensors. The random error could be quite large if the coherence values are not close to unity and/or not a large number of averages are taken [2]. In this work, it was observed that all the coherence values

(Figs. 4, 13 and 14) are very close to unity except in some initial frequencies. On the other hand, quite large number of averages (200) was considered. It could therefore be expected that random error due to phase mismatch would be marginal. The investigation of finite difference, random and bias error is beyond the scope of this study. Useful suggestions in this direction are given by Shibata [33]. It was stated before that the end damping ensured the plates with fully propagating waves, suggesting the reactive and reverberant energy was not disturbing. Considering all of the above points, It may reasonably be argued that phase error does not play a significant role. If the reverse is true, phase error cancellation property of the frequency response technique would be employed [2]. In addition, Hanning window was considered for data acquisition so as to get better solution of leakage.

In this research, both vibration power and vibration amplitude of corrugated plates are compared with that of the isotropic plate. The far-field power, compared for different plate models, is shown in Figs. 25 and 26. This would ensure the effects of rigidity on energy transfer as same input excitation was provided to all plates. The case of designing of any engineering structures under dynamic load, peak response value should be considered. In this paper, consideration should be based on the average value of energy transfer. Depending on this criterion and considering the information in these figures, it is shown that vibration power flow is reduced in the case of corrugated plate in comparison to isotropic plate. A more fruitful comparison would however be possible by plotting the values of far-field power ratio for different plates (Fig. 27). The value of flexural rigidity for isotropic plate (7.684 N m) was less than the rigidities of corrugated plates (7606.775 N m for SRCP and 94.424×10^3 N m for BRCP). From these figures, it is observed that with the increase of flexural rigidity, vibration power flow reduces. This outcome is supported by the results of the graphs of Fig. 28. Frequency response function of acceleration of small rectangular corrugated plate is reduced to that of isotropic plate. Higher stiffness enhances more damping, thereby reducing the amplitude of vibration (Fig. 28) and structural intensity (Fig. 27). Surface treatment on the surface of the plate also reduces the vibration amplitude, Fig. 29. This research directs this distinct way of controlling flexural waves in

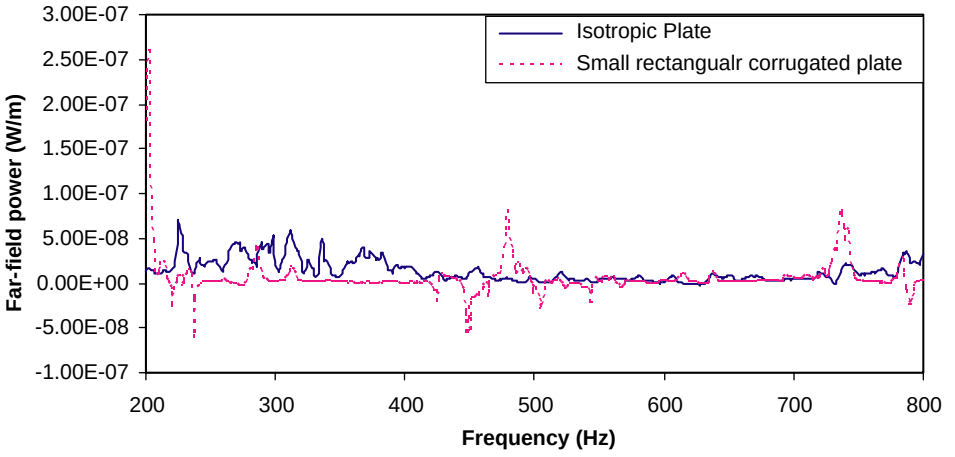

Fig. 25. Comparison of far-field power from isotropic plate and SRCP, upper measurement line, frequency resolution 1 Hz.

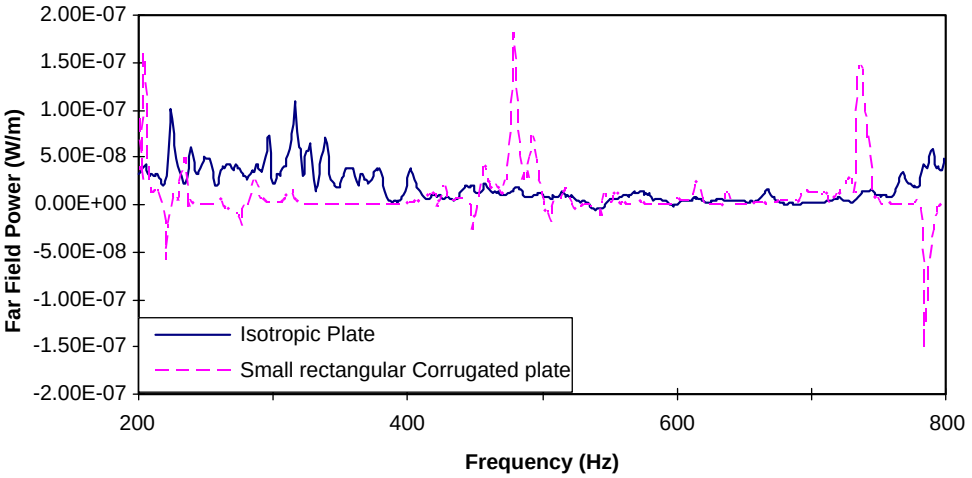

Fig. 26. Comparison of far-field power from isotropic plate and SRCP, lower measurement line, frequency resolution 1 Hz.

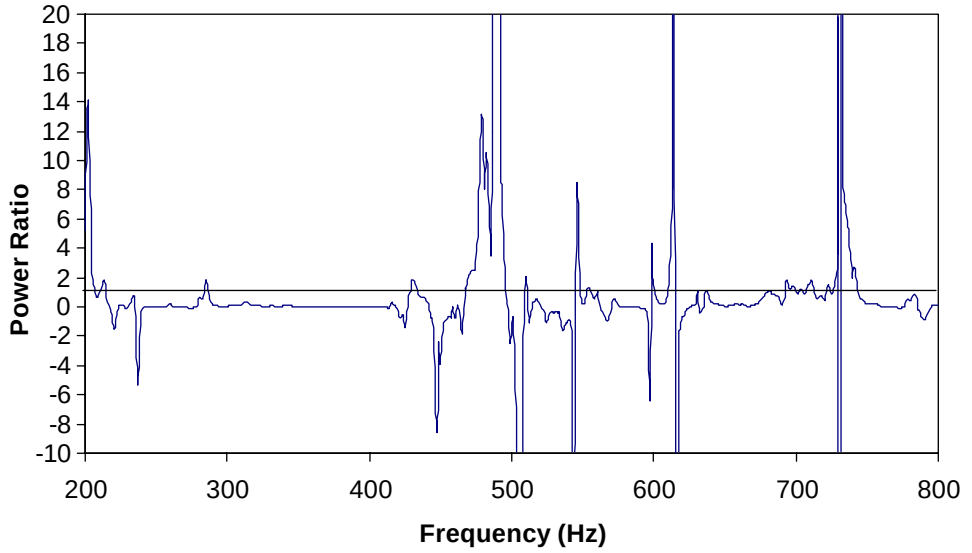

Fig. 27. Power ratio of far-field power (SRCP to isotropic plate) from upper measurement line.

structures. Other than controlling of vibration sources by isolating it from the structure, a passive method of controlling it by increasing flexural rigidity of the structure gives a way not only to reduce vibration amplitude but also reduce vibration energy transfer through plates. As higher rigidity of plates ensures more damping, more vibration energy is absorbed in the plates thereby less acoustic power radiation to the surroundings.

The outcome of reducing vibration power flow and vibration amplitude with the increase of flexural rigidity could ensure an efficient way, a passive means, to control noise and vibration in industries. The increase of flexural rigidity by corrugation of the plates does not result in any

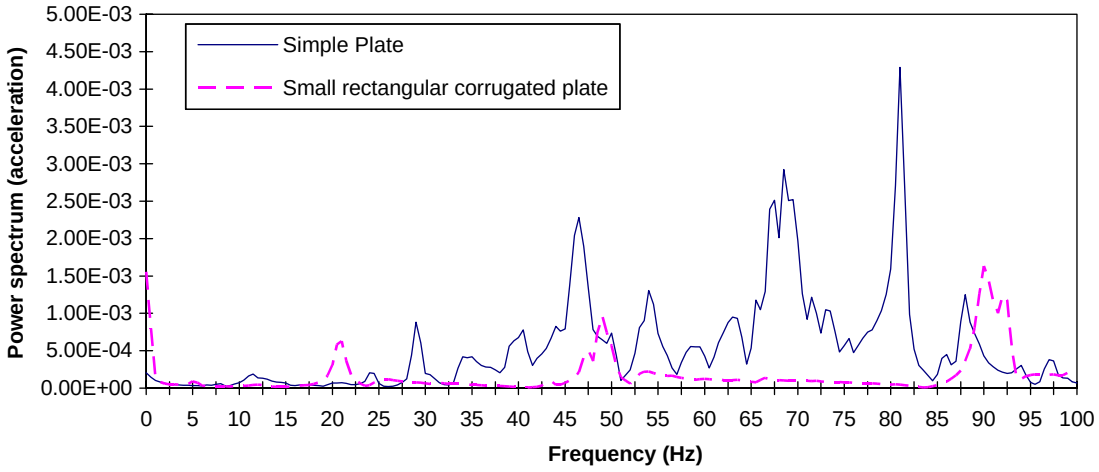

Fig. 28. Measurement of response from isotropic plate and SRCP, resolution of 0.5 Hz.

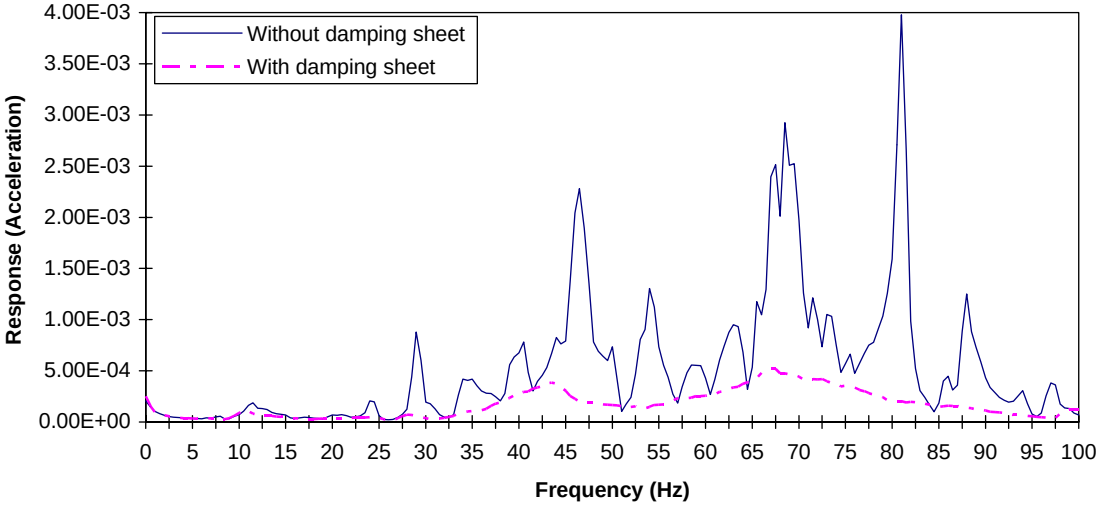

Fig. 29. Response of simple isotropic plate with or without damping sheet (self adhesive heavy bitumen lads with aluminum coating), resolution of 0.5 Hz.

major increase in mass of the plate. To increase same amount of stiffness by increasing the thickness of the plate or stiffening with other beams would surely yield more mass of the plate than that of the corrugation. Corrugation of plate is therefore an effective controlling method of vibration power and vibration amplitude for flexural waves. Effects of rigidity by sinusoidal corrugation and trapezoidal corrugation create more attention now to investigate its influence on vibration energy transfer.

Through the literature search on vibration power flow, it is evident that measurement model has been developed mainly to simple structures. Structural intensity is however available to

naturally orthotropic plates [19]. But no method has been noticed so far which is useful for experimental investigation in technically orthotropic plates. Therefore, a method of elastic equivalence was used to use the method [19] to corrugated plates. This is another objective of this study to investigate the effectiveness of method of elastic equivalence. The similarity of far-field power transmission, input power and their comparison in isotropic plate (without elastic equivalence) and orthotropic plates (with elastic equivalence) would certainly ensure the soundness of the method [7,8]. This ensures its creativity and is considered to be an extension of related works of structural intensity in the literature.

5. Conclusions

In this study, two-transducer method applicable for naturally orthotropic plates is used for estimating vibration energy transfer in technically orthotropic plates. As a result, method of elastic equivalence is used. First the measurements were carried out in an isotropic plate to verify and prove the soundness of methodology and instrumentation and thereby it extends to corrugated plates. The research not only illustrates the usability of two-transducer method [19] to corrugated plates, but also shows how effective is the usage of corrugated plates in controlling flexural waves. It is confirmed that the method of elastic equivalence is an effective way to model corrugated plates. It also ensures that the higher the rigidity of the plate, the lower the vibration energy transmission. As rigidity of the plates increases, vibration amplitudes of it also decreases, thereby acoustic radiation reduces. This is a wonderful way of controlling structure-borne sound without any major weight penalty.

Appendix A. Calculation of flexural wave lengths for different plates

Calculation of flexural wave length for plates requires values of material properties such as Young's Modulus, Poisson's ratio and other dimensions such as thickness, length of repeating section (d_1), mass per unit area (m″), flexural rigidity of the plate and frequency. The basic equations for calculation of flexural wave length are given below:

$$k = \sqrt[4]{\frac{\omega^2 m''}{D_x}}, \tag{A.1}$$

$$\lambda = \frac{2\pi}{k}, \tag{A.2}$$

where k is the flexural wavenumber, ω is the angular frequency, λ is the flexural wave length and D_x is the flexural rigidity of the corrugated plates in the x-direction. If D_x is replaced by D, the flexural rigidity of the isotropic plate, the Eq. (A.1) could be useful for isotropic plates. From Eqs. (A.1) and (A.2), the final form of flexural wave length equation could be manipulated as

$$\lambda^2 = \frac{2\pi}{f}\sqrt{\frac{D_x}{m''}}, \tag{A.3}$$

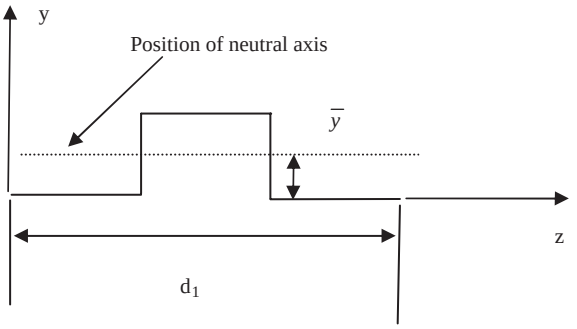

Fig. 30. Position of neutral axis of one repeating section of rectangular corrugated plate, indicating coordinate system.

Table 3
Table for flexural wave lengths for different plates, one isotropic plate and other two rectangular corrugated plates

Types of plate	Neutral axis (mm)	D_x or D (Nm)	λ for 800 Hz (mm)	d/λ
Isotropic plate	—	7.684	96.10	0.2
SRCP	6.125	7606.775	507.04	0.04
BRCP	20.56	94.424×10^3	902.34	0.02

where f is the frequency of the analysis. To calculate D_x for corrugated plates, it is necessary to evaluate the position of neutral axis (Fig. 30) and moment of inertia about its neutral axis [26]. Above table (Table 3) shows the related information for flexural wave length of the plates.

Reference

[1] G. Pavic, Determination of sound power-flow in structures: principles and problems of realization, *Proceeding of International Congress on Recent Developments in Acoustic Intensity Measurements*, CETIM, Senlis France, 1981, pp. 209–215.
[2] J. Linjama, Propagation of mechanical vibration in structure, experimental development of the vibration intensity method, VTT Publication 170, Technical Research Centre of Finland, 1994.
[3] D.U. Noiseux, Measurement of power flow in uniform beams and plates, *Journal of the Acoustical Society of America* 47 (1) (1970) 238–247.
[4] K.Q. Kay, D.C. Swanson, Error in bending wave power measurements, *Noise Control Engineering Journal* 44 (4) (1996) 185–192.
[5] G. Pavic, Measurement of structure borne wave intensity, part I: Formulation of the methods, *Journal of Sound and Vibration* 49 (2) (1976) 221–230.
[6] J.W. Verheij, Cross-spectral density methods for measuring structure borne power flow on beams and pipes, *Journal of Sound and Vibration* 70 (1) (1980) 133–138.
[7] J. Linjama, T. Lahti, Estimation of bending wave intensity in beams using the frequency response technique, *Journal of Sound and Vibration* 153 (1) (1992) 21–36.
[8] P.D. Bauman, Analytical and experimental evaluation of various techniques for the case of flexural waves in one-dimensional structures, *Journal of Sound and Vibration* 174 (5) (1994) 677–694.

[9] J.R.F. Arruda, J.P. Campos, Experimental determination of flexural power flow in beams using a modified prony method, *Journal of Sound and Vibration* 197 (3) (1996) 309–328.
[10] K.Y. Lam, K.M. Liew, S.T. Chow, Study on flexural vibration of triangular composite plates influenced by fibre orientation, *Composite Structures* 13 (1989) 123–132.
[11] K.M. Liew, K.Y. Lam, S.T. Chow, Two-dimensional orthogonal polynomials for vibration of rectangular composite plates,, *Composite Structures* 13 (1989) 239–250.
[12] K.M. Liew, Vibration of symmetrically laminated cantilever trapezoidal composite plates, *International Journal of Mechanical Science* 34 (1992) 299–308.
[13] K.M. Liew, A hybrid energy approach for vibration modeling of laminated trapezoidal plates with point supports, *International Journal of Solids and Structures* 29 (1992) 3087–3097.
[14] K.M. Liew, Vibration of clamped circular symmetric laminates, *ASME Journal of Vibration and Acoustics* 116 (1994) 141–145.
[15] L. Gavric, G. Pavic, A finite element method for computation of structural intensity by the normal mode approach, *Journal of Sound and Vibration* 164 (1) (1993) 29–43.
[16] S.A. Hambric, P.D. Taylor, Comparison of experimental and finite element structure-borne flexural wave power measurements for straight beam, *Journal of Sound and Vibration* 170 (5) (1994) 595–605.
[17] S.A. Hambric, Comparison of finite element prediction and experimental measurements of structure-borne power in a T-shaped beam, *Proceeding of Inter-noise* 95 (1995) pp. 685–688..
[18] R.S. Langley, A wave intensity technique for the analysis of high frequency vibration, *Journal of Sound and vibration* 159 (1992) 483–502.
[19] N.K. Mandal, R.A. Rahman, M.S. Leong, Prediction of Structure borne sound in orthotropic plates for far field conditions, *Journal of Vibration and Control* 8 (1) (2002) 3–12.
[20] N.K. Mandal, M.S. Leong, R. A. Rahman Measurement of quasi-longitudinal wave power in thin single-layer naturally orthotropic plates, *International Journal of Acoustics and Vibration* 5 (2) (2000) 106–108.
[21] D. Quinlin, Application of the four-channel technique to the measurement of power flow in structures. *Proceeding of the Second International Congress on Acoustic Intensity CETIM*, Senlis, France, 1985, pp. 227–234.
[22] R.A. Rahman, A study of vibration power flow in fiber-reinforced plastic materials. PhD thesis, University of Technology Malaysia, 1996.
[23] L. Cremer, M. Heckl, *Structure-Borne Sound: Structural Vibration and Sound Radiation at Audio Frequencies*, Springer, Berlin, 1988.
[24] M.S. Troitskey, *Stiffened Plates: Bending, Stability and Vibration*, Elsevier, Amsterdam, 1976.
[25] Y. Zhang, J.A. Mann III, Example of using structural intensity and the force distribution to study vibrating plates, *Journal of the Acoustical Society of America* 99 (1) (1996) 354–361.
[26] D.E. McFarland, An investigation of the elastic stability of corrugated rectangular plates loaded in pure shear, PhD thesis, University of Kansas, USA, 1967.
[27] G. Rasmessen, Structure borne intensity measurement, *Proceeding of Inter-Noise* 94 (3) (1994) 1727–1730.
[28] A.C. Ugural, *Stress in Plates and Shells*, McGraw-Hill, New York, 1981.
[29] N.J. Huffington Jr., V.A. Blackburg, Theoretical determination of rigidity properties of orthogonally stiffened plates, *Journal of Applied Mechanics, Transactions of the ASME* (1956) 15–20.
[30] D.M. Blackketter, A.P. Boresi, Cross Ribbed rectangular plates, *Mechanics of Structures and Machines* 17 (3) (1989) 321–331.
[31] R. Szilard, *Theory and Analysis of Plates: Classical and Numerical Methods*, Englewood Cliffs, New Jursey, 1973.
[32] N. Tanaka, Vibration and acoustic power flow of an actively control thin plate, *Noise Control Engineering Journal* 44 (1) (1996) 23–33.
[33] K. Shibata, M. Kato, N. Takatsu, O. Wakatsuki, K. Kobayashi, Measuring condition and precision of structural intensity, *Proceeding of Inter-Noise 94*, 1994, pp. 1697–1700.